

Road-Shape Recognition Using On-Vehicle Millimeter-wave Radar

Yasuyuki Miyake, Kazuma Natsume, and Koichi Hoshino

Abstract—In this paper, we present a method for estimating road shape using on-vehicle millimeter-wave radar. The radar detects not only the backscatter from vehicles but also from stationary objects such as crash barriers and sound barrier walls that are generally installed along roads. This indicates that we can estimate road shape by collecting information on the distribution of these objects. We adopt the multiple signal classification (MUSIC) algorithm for increasing the azimuth resolution. Moreover, to apply the MUSIC algorithm into real-time radar systems, the computational cost is reduced by introducing the technique of bi-iteration singular value decomposition (Bi-SVD). The estimated road shapes exhibit good agreement with the actual shapes. Therefore, this technique is expected to improve the reliability of driving support systems.

I. INTRODUCTION

RECENTLY, driving support systems such as adaptive cruise control (ACC) systems and collision mitigation (CM) systems have been introduced into the market. These systems include the use of millimeter-wave radar because such radar is not hampered by fog, rain, snow or other harsh weather conditions [1]. To increase the reliability of these systems, it is crucial to know whether or not a detected object is in the same lane as the host vehicle. To obtain this information, road-shape recognition is necessary. Thus far, road-shape recognition has been studied with vision sensors or laser radar [2], [3]. These sensors have high resolution compared to millimeter-wave radar. However, their performance can become degraded by bad weather conditions. In the end, developing a road-shape recognition system with a robust sensor such as millimeter-wave radar can lead to improved reliability of driving support systems.

The radar detects not only the backscatter from vehicles but also from stationary objects such as crash barriers and sound barrier walls that are located along the road. Therefore, such a system has the possibility of being a platform for road-shape recognition. To realize this road-shape recognition system with radar, the azimuth resolution must be improved. We adopted the multiple signal classification (MUSIC) algorithm for estimating object azimuth. The MUSIC algorithm improves the resolution; however, it has been difficult to apply it into real-time radar systems due to the large computational cost involved. Therefore, we introduced the bi-iteration singular value decomposition (Bi-SVD) technique into the MUSIC algorithm. Bi-SVD is one of various subspace tracking methods, and is used to update only eigenvectors of the signal's subspace [4]. Therefore, using Bi-SVD enables the computational cost in calculating the MUSIC algorithm to be reduced. Furthermore,

we adopted a frequency modulated continuous wave (FM-CW) system that detects range and relative speed simultaneously. This enables us to extract stationary objects much easier by comparing their relative speed with the ground speed.

In this paper, we suggest a road-shape recognition system with a millimeter-wave radar. In this system, the Bi-SVD-based MUSIC algorithm is introduced into the azimuth estimation. We demonstrated the recognition performance on an actual radar system.

II. SUBSPACE-BASED HIGH-RESOLUTION ALGORITHM

A. Multiple Signal Classification

We adopted an N -element uniform linear array antenna for estimating object azimuth. Let $\mathbf{x}(t) = [x_1(t), x_2(t), \dots, x_N(t)]^H$ be the data vector observed at discrete time of t . It consists of N components that are outputs from each antenna element, and is represented by

$$\mathbf{x}(t) = \mathbf{A}\mathbf{s}(t) + \mathbf{n}(t) \quad (1)$$

where $\mathbf{A} = [\mathbf{a}(\mu_1), \mathbf{a}(\mu_2), \dots, \mathbf{a}(\mu_L)]$ is an $N \times L$ direction-of-arrival (DOA) matrix with L arriving signals, $\mathbf{s}(t) = [s_1(t), s_2(t), \dots, s_L(t)]^T$ is a source vector, and $\mathbf{n}(t)$ is a white noise vector with equal variance of σ^2 . The vectors of $\mathbf{a}(\mu) = [1, e^{j\mu}, \dots, e^{j(N-1)\mu}]^H$ are the steering vectors, where

$$\mu = \frac{2\pi d \sin \theta}{\lambda}. \quad (2)$$

In (2), d is the space between adjacent antenna elements, λ is the wavelength, and θ is the DOA. Then, the correlation matrix is given by

$$\begin{aligned} \mathbf{R}_{xx} &= \mathbf{A}E[\mathbf{s}(t)\mathbf{s}^H(t)]\mathbf{A}^H + E[\mathbf{n}(t)\mathbf{n}^H(t)] \\ &= \mathbf{A}\mathbf{S}\mathbf{A}^H + \sigma^2\mathbf{I} \end{aligned} \quad (3)$$

where $E[\cdot]$ denotes the expectation and \mathbf{I} is the identity matrix. Let λ_i and \mathbf{e}_i ($i = 1, \dots, N$) denote the eigenvalues and the corresponding eigenvectors of \mathbf{R}_{xx} . λ_i have the following relation as:

$$\lambda_1 \geq \dots \geq \lambda_L > \lambda_{L+1} = \dots = \lambda_N = \sigma^2. \quad (4)$$

The eigenvectors are divided into two groups that are based

on whether or not the corresponding eigenvalues are equal to σ^2 . Eigenvectors whose corresponding eigenvalues are larger than σ^2 are referred to as signal eigenvectors. On the other hand, eigenvectors whose corresponding eigenvalues are equal to σ^2 are referred to as noise eigenvectors. Normally, a signal subspace matrix \mathbf{E}_S and noise subspace matrix \mathbf{E}_N are defined as

$$\mathbf{E}_S = [\mathbf{e}_1, \mathbf{e}_2, \dots, \mathbf{e}_L] \quad (5)$$

$$\mathbf{E}_N = [\mathbf{e}_{L+1}, \mathbf{e}_{L+2}, \dots, \mathbf{e}_N]. \quad (6)$$

\mathbf{E}_S is the orthogonal complement of \mathbf{E}_N . Therefore we have the relation as follows:

$$\mathbf{E}_S \mathbf{E}_S^H + \mathbf{E}_N \mathbf{E}_N^H = \mathbf{I}. \quad (7)$$

It is easy to verify that the steering vectors and noise eigenvectors are orthogonal to each other. Based on this relation, the MUSIC spectrum is given by

$$P_{MUSIC}(\theta) = \frac{\mathbf{a}^H(\theta)\mathbf{a}(\theta)}{\mathbf{a}^H(\theta)\mathbf{E}_N\mathbf{E}_N^H\mathbf{a}(\theta)}. \quad (8)$$

B. Bi-iteration Singular Value Decomposition

The \mathbf{E}_N in (8) is generally calculated using batch eigenvalue decomposition (ED). However, this is very time consuming. Therefore, thus far it has been difficult to incorporate the MUSIC algorithm into real-time applications such as radar systems. To overcome this difficulty, we introduced Bi-SVD, one of various subspace tracking techniques, into the MUSIC algorithm. This technique updates only the signal subspace matrix, so therefore saves considerable computation time compared to using ED. Moreover, because past data are preserved in the successive calculation, we can obtain stable spectrum. In the following, we will describe the Bi-SVD technique. Let $\mathbf{X}(t)$ be an $N \times M$ data matrix (M : number of all snapshots), which is defined as

$$\mathbf{X}(t) = [\alpha^{1/2}\mathbf{X}(t-1) \quad (1-\alpha)^{1/2}\mathbf{x}(t)] \quad (9)$$

where $\mathbf{X}(t-1)$ is the previous data matrix and α ($0 < \alpha < 1$) is the forgetting factor. Correlation matrix $\mathbf{R}_{xx}(t)$ at discrete time of t is given by

$$\begin{aligned} \mathbf{R}_{xx}(t) &= \mathbf{X}(t)\mathbf{X}^H(t) \\ &= \alpha\mathbf{R}_{xx}(t-1) + (1-\alpha)\mathbf{x}(t)\mathbf{x}^H(t). \end{aligned} \quad (10)$$

The value of α should be carefully chosen, because the MUSIC spectrum can differ widely with varying values. The eigenvectors of $\mathbf{R}_{xx}(t)$ are equivalent to the right singular vectors that are calculated from $\mathbf{X}(t)$ with singular value decomposition (SVD). Bi-SVD is a technique that performs

SVD with the following bi-iteration:

$$\mathbf{Q}_A(0) = \begin{bmatrix} \mathbf{I}_L \\ \mathbf{0} \end{bmatrix} \quad (11)$$

$$\mathbf{B}(t) = \mathbf{X}^H(t)\mathbf{Q}_A(t-1) \quad (12)$$

$$\mathbf{B}(t) = \mathbf{Q}_B(t)\mathbf{R}_B(t) \quad (13)$$

$$\mathbf{A}(t) = \mathbf{X}(t)\mathbf{Q}_B(t) \quad (14)$$

$$\mathbf{A}(t) = \mathbf{Q}_A(t)\mathbf{R}_A(t). \quad (15)$$

$\mathbf{Q}_A(t)$ is a $N \times L$ recursion matrix that will converge the signal subspace. $\mathbf{R}_A(t)$ and $\mathbf{R}_B(t)$ are $L \times L$ upper triangular matrices and they will converge the diagonal matrix of L dominant singular values of $\mathbf{X}(t)$. $\mathbf{Q}_B(t)$ is the $M \times L$ recursion matrix that consists of orthonormal columns. To perform (10)–(14), the definition of low-rank approximation is introduced:

$$\mathbf{X}^H(t) \approx \mathbf{Q}_B(t)\mathbf{R}_B(t)\mathbf{Q}_A^H(t-1). \quad (16)$$

An L -dimensional compressed dimensional data vector $\mathbf{h}(t)$, an $L \times L$ cosine matrix $\mathbf{\Theta}_A(t)$, and an orthogonal projection data vector are defined as follows:

$$\mathbf{h}(t) = \mathbf{Q}_A^H(t-1)\mathbf{x}(t) \quad (17)$$

$$\mathbf{\Theta}_A(t) = \mathbf{Q}_A^H(t-1)\mathbf{Q}_A(t) \quad (18)$$

$$\mathbf{x}_\perp(t) = \mathbf{x}(t) - \mathbf{Q}_A^H(t-1)\mathbf{h}(t). \quad (19)$$

The time update for the signal subspace $\mathbf{Q}_A(t)$ is given by

$$\mathbf{Q}_A(t) = \mathbf{Q}_A(t-1)\mathbf{\Theta}_A(t) + \mathbf{x}_\perp(t)\mathbf{f}^H(t) \quad (20)$$

where

$$\mathbf{f}(t) = \mathbf{Q}_A^H(t)\mathbf{x}_\perp(t). \quad (21)$$

Considering the relation in (7), the MUSIC spectrum at discrete time of t is given by

$$P_{MUSIC}(\theta, t) = \frac{\mathbf{a}^H(\theta)\mathbf{a}(\theta)}{\mathbf{a}^H(\theta)\{\mathbf{I} - \mathbf{Q}_A(t)\mathbf{Q}_A^H(t)\}\mathbf{a}(\theta)}. \quad (22)$$

C. Music Spectrum

In this section, we describe the performance of object azimuth estimation using the MUSIC algorithm. The estimation is done with data collected by a millimeter-wave radar. Five antenna elements are used to estimate the object azimuth. Fig. 1 illustrates the conditions under which we collected the data. Two corner-reflectors are placed at the same distance of 17 m from a host vehicle with radar installed. The reflectors are spaced 3.0 m apart from each other. Fig. 2 shows the calculated MUSIC spectrum that is corresponding to the situation as shown in Fig. 1. The spectral peaks of the MUSIC algorithm match the directions of the reflector. The

DOA estimation results calculated with beamforming (BF) and estimation of signal parameters via rotational invariance technique (ESPRIT) [5] are also plotted. In this situation, both BF and ESPRIT give the same estimation results. However, the resolution of the BF is not enough for automotive applications. On the other hand, the resolution of the ESPRIT is equivalent to the MUSIC algorithm. However, TLS-ESPRIT type algorithms [6] require operations of at least three SVDs. That prevents it from being adopted in real-time applications.

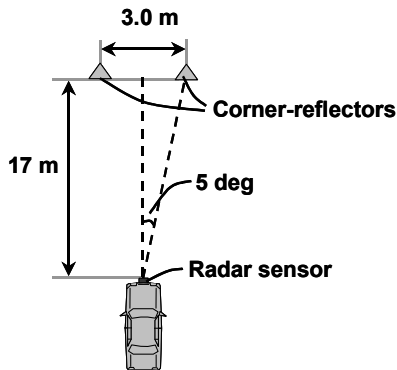


Fig. 1. Conditions under which data collection was performed for estimating object positions using the MUSIC algorithm. Two corner-reflectors are placed at the same distance of 17 m.

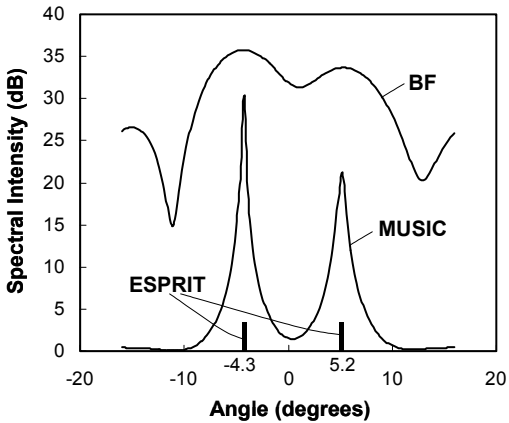


Fig. 2. DOA estimation results calculated with MUSIC, BF and ESPRIT. Vertical and horizontal axes represent spectral intensity and angle, respectively.

D. Calculation-Time

The MUSIC algorithm requires operations of one SVD to obtain the spectrum. This means that it still has large computational cost that should be reduced. Therefore we introduced the Bi-SVD technique into the MUSIC algorithm. Table I shows operation counts for the Bi-SVD and standard SVD technique. It should be noted that the numbers of

arriving signal of 2 is used in the count estimations. When the Bi-SVD technique is introduced, the calculation time is reduced approximately 45%. In this case, the calculation was done with Pentium-based Visual C++ software.

TABLE I
OPERATION COUNTS FOR BI-SVD AND SVD METHOD

	Bi-SVD	SVD
Multiplications	928	3335
Additions	926	3335

III. RADAR IMAGE

In this chapter, we describe a radar image that is used in the process of road-shape recognition. The radar image is an intensity graph that consists of the MUSIC spectra calculated over all beat frequencies. Fig. 3 shows the obtained radar image at the moment corresponding to the upper photograph. We can see a few vehicles moving on the road. A sound barrier wall and crash barrier are seen on the left and right sides, respectively. The ground speed of the host vehicle was 95 km/h at that moment. The left curved line in the radar image corresponds to the backscatter from the sound barrier wall, and the shorter curved line on the right corresponds to the backscatter from the crash barrier. The backscatter from vehicles is also detected. The circled peak relates to the backscatter from Vehicle 1, which is moving in the same lane as the host vehicle. The dotted circle relates to the backscatter from Vehicle 2, which is moving in the adjacent lane. The ranges of Vehicle 1 and Vehicle 2 are 67 m and 85 m, respectively. We calculated the radar image over both up-chirp and down-chirp regions of the FM-CM system.

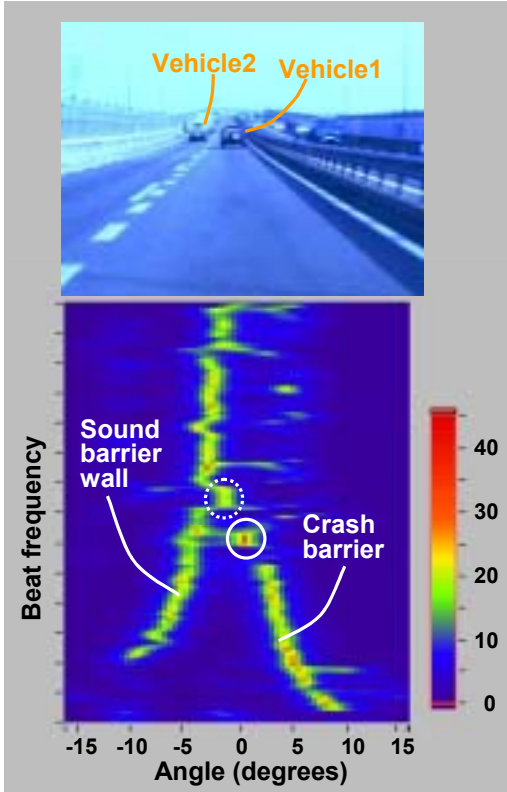


Fig. 3. Calculated radar image using the Bi-SVD technique. The radar image was obtained at the moment of the upper photograph. The horizontal and vertical axes represent angle and beat frequency, respectively.

IV. ROAD-SHAPE RECOGNITION

Next, we describe the method for extracting the road shape from the obtained radar image. First, we extracted the spectral peaks from the radar image. As mentioned above, the radar detects not only backscatter from stationary objects but also backscatter from moving objects such as vehicles. Therefore, we had to eliminate these from the image. Considering that the relative speed of any stationary object is equal to the ground speed of the host vehicle, these can be extracted by observing their relative speed. After extracting the peaks, they are transformed into Cartesian coordinates. Then the road curvature and x -axis intercept point were extracted by the Hough transform technique. We defined a 2nd ordered polynomial model given by

$$x = ay^2 + b \quad (23)$$

where a and b are the road curvature and intercept point, respectively. Position (x, y) is the coordinate of the stationary object. Equation (23) is transformed into a 2-dimensional parameter space, as follows:

$$b = -y^2 a + x \quad (24)$$

Each position (x, y) of the stationary object generates one line in the parameter space. Then, plural lines are placed onto the space. The intersection of these lines indicates the coordinate most suitable as a parameter pair for the polynomial curve. If we vote the lines to the parameter space, the local maximum is formed around the intersection. The voting result corresponding to the radar image is shown in Fig. 4. Two local maximums are clearly observed in the parameter space. These correspond to the left and right road edges.

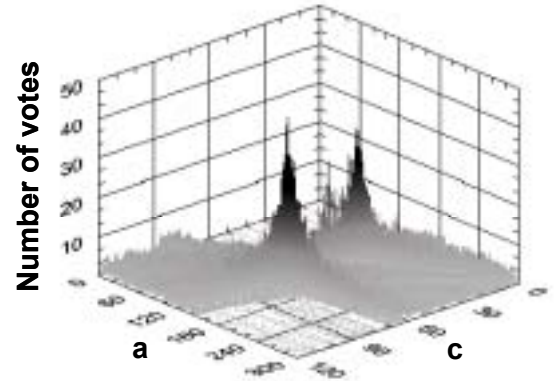


Fig. 4. Voting result corresponding to the radar image in Fig. 3. Axes a and c represent the curvature and x intercept, respectively.

We tracked the road shapes using a Kalman Filter based on a clothoid road model. The state vector of the model is given by

$$s = [c_0 \quad c_1 \quad b] \quad (25)$$

where c_0 and c_1 are the road curvature and the rate of the curvature change, respectively. b is the x -axis intercept point. The c_0 and c_1 have the following relations:

$$\dot{c}_0 = \nu c_1 \quad (26)$$

$$\dot{c}_1 = 0. \quad (27)$$

ν is the ground speed of the host vehicle.

V. RESULTS

The estimated road shapes corresponding to the moment illustrated in Fig. 3 are shown in Fig. 5, which also plots the extracted stationary objects. The solid lines and square dots denote the estimated road shapes and stationary objects, respectively. Most of the peaks corresponding to vehicles

moving in front of the host have been eliminated. The estimated road shapes exhibited good agreement with the actual shapes.

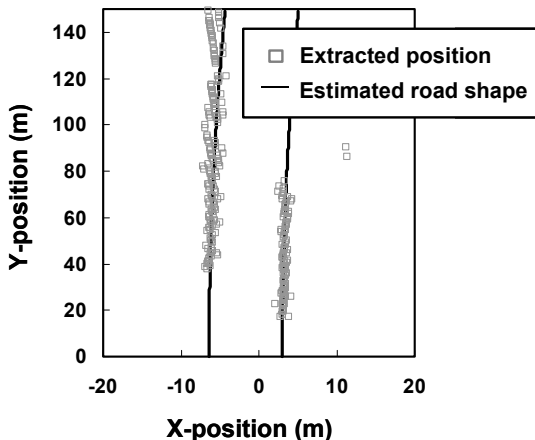


Fig. 5. Estimated road shapes and positions of extracted stationary objects on a curved road. Solid lines and square dots represent the road shapes and positions of the stationary objects, respectively.

Next we demonstrate the road-shape recognition performance when the host vehicle moves on the road whose radius is 160 m. Fig. 6 shows the estimated road shapes and extracted stationary objects at the moment corresponding to the upper photograph. In the photo we see a sound barrier wall whose height is approximately 3.0 m. Backscatter from the wall is comparatively large because the wall is partially made of metal. The estimated road shapes also exhibited good agreement with the actual shapes. It should be noted that only the road edge on the right side was extracted in this situation. This is because the left wall is out of range for radar detection. Fig. 7 shows the tracked road curvature at the road. The absolute curvature gradually increased up to 0.6×10^{-3} and then decreased. This tracked curvature well described the actual situation.

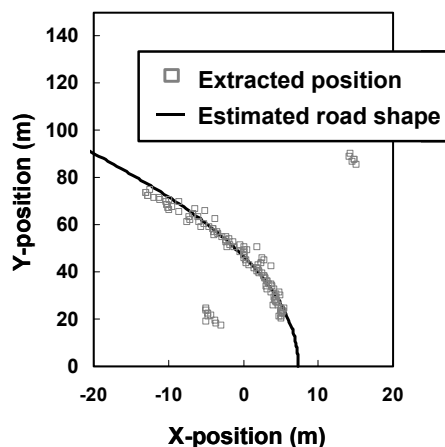


Fig. 6. Estimated road shape and positions of extracted stationary objects on a curved road

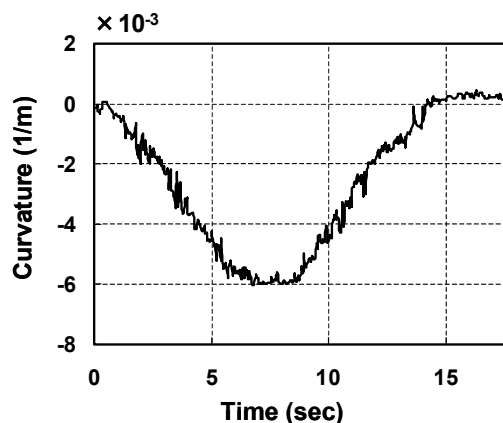


Fig. 7. Tracked road curvature

VI. CONCLUSION

We demonstrated here the performance of road-shape recognition with millimeter-wave radar. To increase the azimuth resolution, the Bi-SVD-based MUSIC algorithm was introduced. The tracked road shapes exhibited good agreement with the actual shapes, even if some vehicles were moving in front of the host. The computational cost in calculating the MUSIC algorithm was reduced 45% for

application into a real-time radar system. From the standpoint of sensor robustness, a radar system such as this is expected to be a platform for road-shape recognition and to increase the reliability of driving support systems.

ACKNOWLEDGMENTS

The authors would like to thank Y. Sakuma and Y. Watanabe of DENSO CORPORATION, and C. Yamano and H. Shirai of DENSO IT LABORATORY for their technical assistance and useful discussions.

REFERENCES

- [1] Y. Miyake, Y. Watanabe, and K. Natsume, "Automotive Radar with High-resolution Algorithm," Proceedings of the 13th ITS World Congress (London), Oct. 2006.
- [2] Y. Wang, D. Shen, and E. K. Teoh, "Lane detection using a spline model," Pattern Recognition Letters, Vol. 21, pp. 677–689, 2000.
- [3] T. Ogawa and K. Takagi, "Lane Recognition Using On-vehicle LIDAR," IEEE Symp. on Intelligent Vehicles, pp. 540–545, 2006.
- [4] P. Strohoch, "Bi-Iteration SVD Subspace Tracking Algorithms," IEEE Trans. Signal Processing, Vol. 45, pp. 1222–1240, May 1997.
- [5] N. Kikuma, "Iterative DOA estimation using subspace tracking methods and adaptive beamforming," IEIEC Trans. Commun., Vol.E88-B, No. 5, pp.1818–1828, May 2005.
- [6] B. Ottersten, M. Viberg, and T. Kailath, "Performance analysis of the total least squares ESPRIT algorithm," IEEE Trans. Signal Process., Vol.39, No. 5, pp.1122–1135, May 1991.